A cell-active inhibitor of mitogen-activated protein kinase phosphatases restores paclitaxel-induced apoptosis in dexamethasone-protected cancer cells

Andreas Vogt,[1,3,4] Peter R. McDonald,[1,3] Aletheia Tamewitz,[1] Rachel P. Sikorski,[1] Peter Wipf,[2,3,4] John J. Skoko III,[1,3] and John S. Lazo[1,3,4]

Departments of [1]Pharmacology and [2]Chemistry, [3]University of Pittsburgh Drug Discovery Institute, and [4]Pittsburgh Molecular Libraries Screening Center, University of Pittsburgh, Pittsburgh, Pennsylvania

Abstract

Mitogen-activated protein kinase phosphatase (MKP)-1 is a dual-specificity phosphatase that negatively regulates the activity of mitogen-activated kinases and that is overexpressed in human tumors. Contemporary studies suggest that induction of MKP-1 during chemotherapy may limit the efficacy of clinically used antineoplastic agents. Thus, MKP-1 is a rational target to enhance anticancer drug activity, but suitable small-molecule inhibitors of MKP-1 are currently unavailable. Here, we have used a high-content, multiparameter fluorescence-based chemical complementation assay for MKP activity in intact mammalian cells to evaluate the cellular MKP-1 and MKP-3 inhibitory activities of four previously described, quinone-based, dual-specificity phosphatase inhibitors, that is, NSC 672121, NSC 95397, DA-3003-1 (NSC 663284), and JUN-1111. All compounds induced formation of reactive oxygen species in mammalian cells, but only one (NSC 95397) inhibited cellular MKP-1 and MKP-3 with an IC_{50} of 13 μmol/L. Chemical induction of MKP-1 by dexamethasone protected cells from paclitaxel-induced apoptosis but had no effect on NSC 95397. NSC 95397 phenocopied the effects of MKP-1 small inhibitory RNA by reversing the cytoprotective effects of dexamethasone in paclitaxel-treated cells. Isobologram analysis revealed synergism between paclitaxel and NSC 95397 only in the presence of dexamethasone. The data show the power of a well-defined cellular assay for identifying cell-active inhibitors of MKPs and support the hypothesis that small-molecule inhibitors of MKP-1 may be useful as antineoplastic agents under conditions of high MKP-1 expression. [Mol Cancer Ther 2008;7(2):330–40]

Received 10/4/07; accepted 11/12/07.

Grant support: NIH grants CA52995 and CA78039 and Fiske Drug Discovery Fund.

The costs of publication of this article were defrayed in part by the payment of page charges. This article must therefore be hereby marked *advertisement* in accordance with 18 U.S.C. Section 1734 solely to indicate this fact.

Requests for reprints: John S. Lazo, Department of Pharmacology, University of Pittsburgh, Biomedical Science Tower 3, 3501 Fifth Avenue, Pittsburgh, PA 15260. Phone: 412-648-9200; Fax: 412-648-9009. E-mail: lazo@pitt.edu

doi:10.1158/1535-7163.MCT-07-2165

Introduction

Mitogen-activated protein kinase (MAPK) phosphatases (MKP) dephosphorylate MAPKs on threonine and tyrosine residues. MAPKs have a pivotal role in mitogenic signal transduction, survival, stress response, and programmed cell death (1). Extensive studies on the activation of MAPK pathways by upstream kinases and cell-surface receptor-mediated events have revealed MAPK signal transduction cascades as pivotal members in an intricate signaling network. In contrast, the events that regulate termination of MAPK signaling are less well understood, although MKPs clearly play a major role (2). To date, 12 human MKPs have been identified, which possess unique but overlapping substrate specificities and whose activity and expression is regulated on multiple levels (1), including induction by extracellular stimuli (3), protein stabilization (4), and destabilization (5).

Within the MKP family, MKP-1 appears to play an important role in tumorigenesis (reviewed in ref. 6). Evidence that MKP-1 may actually support the transformed phenotype comes from a study by Liao et al. who showed that PANC-1 human pancreatic cancer cells stably transfected with a full-length MKP-1 antisense construct had longer doubling times, decreased ability to form colonies in soft agar, and loss of tumorigenicity in nude mice (7). Ectopic overexpression of MKP-1 has been reported to protect cells from the cytotoxic effects of UV irradiation (8) and cisplatin (9, 10). Up-regulation of MKP-1 can protect cells against apoptosis induced by paclitaxel (11, 12), proteasome inhibitors (13), and radiation therapy (14).

Although MKP-1 may be an important regulator of the malignant phenotype, optimal small-molecule inhibitors of MKP-1 are lacking. Such compounds might not only be useful for improving the efficacy of antineoplastic agents under conditions of high MKP-1 expression but would also be valuable to probe the biochemical substrates and functionality of MKP-1. Although we have identified several pharmacophores with *in vitro* activity against MKP-1 (15–17), few have cellular activities associated with MKP-1 inhibition (17, 18). Currently, the most popular approach to identifying potential phosphatase inhibitors are *in vitro* assays using recombinant enzymes and small-molecule synthetic substrates, such as *p*-nitrophenyl phosphate or *O*-methyl fluorescein phosphate. These small-molecule substrates have been employed because

they provide a robust output signal, are inexpensive, and are more convenient to use than the phosphorylated protein substrate. Nonetheless, we now know that the activity of MKPs depends on their interaction with other proteins in the cell. For example, the enzyme activities of MKP-1, MKP-2, and MKP-3 are substantially enhanced by the activated forms of their respective substrates (19). Thus, *in vitro* screening assays may not be predictive of compound effect within the context of the whole cell.

We reported previously a method to analyze MKP activity in a cellular context. The method, which we have termed ''chemical complementation'' (20), enables an unbiased analysis of MKP activity that does not require knowledge about structure, binding partners, or activation state. Using this assay, we discovered a plant alkaloid, sanguinarine, as a cell-active inhibitor of MKP-1 (18). Although sanguinarine was the first reported cell-active small-molecule MKP-1 inhibitor and showed selectivity for MKP-1 over MKP-3 in intact cells, its utility as a biological tool to investigate MKP-1 function is limited because it has several cellular activities that occur at concentrations well below those required to inhibit MKP-1 (21–24).

In this report, we have used the chemical complementation assay to evaluate a panel of previously described, structurally similar, quinone-based DSPase inhibitors for their ability to inhibit cellular MKPs. All compounds produced reactive oxygen species (ROS), but only one of them (NSC 95397) inhibited MKP-1 and MKP-3. Chemical induction of MKP-1 by dexamethasone protected human breast cancer cells against paclitaxel but not NSC 95397. NSC 95397 reversed the cytoprotective effects of dexamethasone in paclitaxel-treated cells, and the combination of paclitaxel and NSC 95397 was synergistic in the presence of dexamethasone. The data suggest that MKP-1 is a primary cellular target of NSC 95397 and support the hypothesis that inhibition of MKP-1 by small molecules is a viable strategy to enhance the efficacy of chemotherapeutic regimens under conditions of high MKP-1 expression.

Materials and Methods

Chemicals

2-(2-Mercaptoethanol)-3-methyl-1,4-naphthoquinone (NSC 672121), 2,3-bis-[2-hydroxyethylsulfonyl]-[1,4] naphthoquinone (NSC 95397), 7-chloro-6-(2-morpholin-4-ylethylamino)-quinoline-5,8-dione (NSC 663284 or DA-3003-1), and 6-(2-morpholin-4-ylethylamino)-quinoline-5,8-dione (JUN-1111) have been described previously (25–28). NSC numbers denote the identity of compounds in the National Cancer Institute's Chemical Repository. 5-(and 6)-Chloromethyl fluorescein diacetate, acetyl ester (CM-H_2-DCFDA) was from Molecular Probes. All other chemicals were from Sigma-Aldrich.

Antibodies and Plasmids

Mouse monoclonal anti-phospho-Erk (E10), rabbit polyclonal phospho-Erk, phospho-JNK, pan-JNK/SAPK, and MKP-1 (C-19) antibodies were from Cell Signaling Technology. Rabbit polyclonal Erk antibody and mouse monoclonal anti-c-myc (9E10) antibodies were from Santa Cruz Biotechnology. Secondary antibodies were Alexa Fluor 488–conjugated goat anti-mouse, Alexa Fluor 647–conjugated anti-rabbit IgG (Molecular Probes), and horseradish peroxidase–conjugated goat-anti rabbit IgG and goat-anti mouse IgG (Jackson ImmunoResearch). cDNA encoding myc-tagged MKP-3 (PYST-1) in a pSG5 mammalian expression vector (29, 30) was a gift from Dr. Stephen Keyse (Cancer Research United Kingdom). A plasmid encoding myc-tagged mouse MKP-1 (1-313) in a pCEP4 mammalian expression vector was a gift from Dr. Nicholas Tonks (Cold Spring Harbor Laboratories). To improve transfection efficiency, a *Bam*HI-*Eco*RI fragment containing the c-myc MKP-1 sequence was excised from the pCEP vector and subcloned into pcDNA3.1 (Clontech).

Cell Culture

Cell lines were obtained from American Type Culture Collection and maintained in a humidified atmosphere of 5% CO_2 at 37°C. HeLa cells were maintained in DMEM. MDA-MB-231 cells were grown in RPMI 1640. All growth media were supplemented with 10% fetal bovine serum (HyClone) and 1% penicillin-streptomycin (Life Technologies).

Chemical Complementation Assay for MKP-1 and MKP-3

HeLa cells (5, 000) were plated in the wells of a collagen-coated 384-well plate (Falcon Biocoat) and allowed to attach overnight. Cells were transfected with c-myc MKP-3, c-myc MKP-1, or enhance green fluorescent protein (GFP) cDNAs (100 ng/well) and LipofectAMINE 2000 (2.5 μL/μg DNA; Invitrogen) in Opti-MEM reduced serum medium as per manufacturer's instructions. Complexes were removed 3.25 h after transfection, and fresh medium containing 10% fetal bovine serum was added. Eighteen hours later, cells were treated in quadruplicate wells for 15 min with phorbol ester (TPA) or mixtures of TPA and phosphatase inhibitors, fixed, and immunostained with a mixture of anti-phospho-Erk (1:200 dilution; Cell Signaling Technology) and anti-c-myc (1:100 dilution; Santa Cruz Biotechnology) antibodies as described (20). Positive phospho-Erk and c-myc MKP signals were visualized with Alexa Fluor 647 (phospho-Erk)–conjugated and Alexa Fluor 488 (c-myc)–conjugated secondary antibodies, respectively. All staining steps were carried out on a Biomek 2000 laboratory automation workstation (Beckman-Coulter).

Plates were analyzed by three-channel multiparametric analysis for phospho-Erk and c-myc MKP intensities in an area defined by nuclear staining using the Compartmental Analysis Bioapplication on the ArrayScan II (Cellomics). Images were acquired in three independent fluorescence channels using an Omega XF93 filter set at excitation/emission wavelengths of 350/461 nm (Hoechst), 494/519 nm (Alexa Fluor 488), and 650/665 nm (Alexa Fluor 647), respectively. At least 1,000 individual cells were analyzed for phospho-Erk, c-myc MKP-3, c-myc MKP-1, or GFP intensities. For each condition, the percentage of MKP (GFP)–expressing cells was determined from FITC (Alexa Fluor 488) intensity distribution histograms, setting appropriate

gates for MKP (GFP)–positive and MKP (GFP)–negative cells. Phospho-Erk levels were then averaged in MKP-expressing and nonexpressing subpopulations. Large positive differences in phospho-Erk intensities between the two subpopulations indicated lower levels of phospho-Erk in MKP-expressing cells compared with nonexpressing cells. Low differences indicated similar levels of phospho-Erk in both cell subpopulations.

Detection and Quantitation of ROS

HeLa cells were grown to confluency on 384-well plates and labeled with Hoechst 33342 (2 μg/mL). Cells were washed with HBSS and loaded with 5 μmol/L CM-H_2-DCFDA for 15 min at 37°C, washed again, and treated with test agents for 10 min at 37°C. After two additional washing steps, cells were analyzed for Hoechst and FITC fluorescence using an Omega XF100 filter set on the ArrayScan II. To quantify ROS generation, a threshold for FITC-positive cells was defined as the average FITC intensity plus 1 SD from six vehicle-treated wells. Cells were classified as positive for ROS if their average FITC intensity exceeded this threshold.

Western Blotting

For the Western blot implementation of the chemical complementation assay, HeLa cells (3×10^5) were plated in six-well plates and transfected with 2 μg plasmids encoding EGFP or c-myc MKP-1 in the presence of LipofectAMINE 2000 (2.5 μL/100 ng DNA). After 3.25 h, transfection medium was replaced by complete growth medium. Cells were allowed to recover overnight and treated with vehicle, TPA, NSC 95397, or a mixture of TPA and NSC 95397 for 30 min. Cell lysates were resolved on 4% to 20% SDS-PAGE gels and transferred to nitrocellulose membranes (Protran, Schleicher & Schuell). Membranes were probed with appropriate primary antibodies. Positive antibody reactions were visualized using peroxidase-conjugated secondary antibodies (Jackson ImmunoResearch) and an enhanced chemiluminescence detection system (Western Lightning, Perkin-Elmer Life Sciences) according to the manufacturer's instructions. For quantitation of protein expression levels, luminescence band intensities were measured on a Kodak i1000 imaging station using a 14-bit CCD camera under nonsaturating conditions (Perkin-Elmer Life Sciences).

Chromatin Condensation

MDA-MB-231 cells (20,000 per well) were plated in collagen-coated 384-well microplates and incubated at 37°C in a 5% CO_2, humidified incubator for 3 to 8 h to allow attachment and spreading. Wells were treated with vehicle (DMSO) or ten 2-fold concentration gradients of test agents and incubated for an additional 20 h at 37°C. Cells were fixed in 4% (v/v) aqueous formaldehyde and nuclei/chromatin were simultaneously labeled with 10 μg/mL Hoechst 33342 in HBSS. Microplates were analyzed with an ArrayScan II using the Compartmental Analysis Bioapplication. Within the application, 1,000 individual cells in each well were imaged using a 10× objective and a Hoechst 33342 compatible filter set. For determination of nuclear condensation, a threshold for nuclear staining intensity was defined as the average Hoechst 33342 intensity plus 1 SD from 28 vehicle-treated wells placed in the center of the

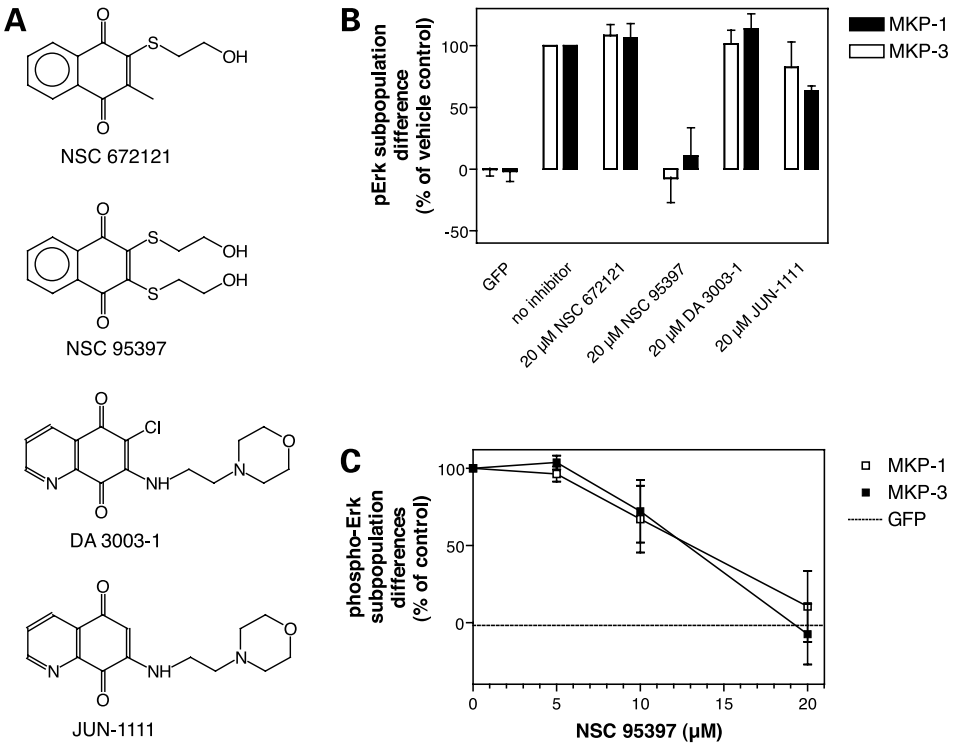

Figure 1. Inhibition of cellular MKP-1 and MKP-3 by quinone-based DSPase inhibitors. **A,** structures of DSPase inhibitors. **B** and **C,** chemical complementation assay for MKP-1 and MKP-3. HeLa cells transfected with c-myc MKP-1 or c-myc MKP-3 were stimulated with TPA in the presence of inhibitors and analyzed for phospho-Erk subpopulation differences as described in Materials and Methods. **B,** at a single concentration (20 μmol/L), only NSC 95397 inhibited MKP-1 and MKP-3. **C,** concentration-dependent inhibition of MKP-1 and MKP-3 by NSC 95397. Data are the averages ± SE from at least three independent experiments.

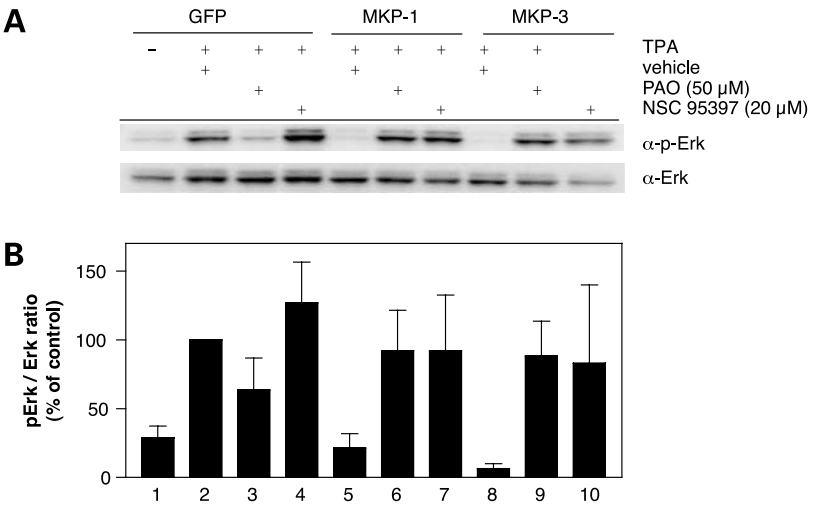

Figure 2. Confirmation of cellular MKP inhibition by NSC 95397 by Western blot analysis. HeLa cells were plated in 100-mm dishes, transfected with GFP (*lanes 1-4*), MKP-1 (*lanes 5-7*), or MKP-3 (*lanes 8-10*), and stimulated with TPA in the presence or absence of NSC 95397 (20 μmol/L) or PAO (50 μmol/L). **A,** lysates were separated on SDS-PAGE and immunoblotted with anti-phospho-Erk (α-*pErk*) or anti-Erk (α-*Erk*) antibodies. *Lane 1,* GFP-transfected and unstimulated control; *lanes 2* to *10,* cells stimulated with TPA and transfected with GFP (*lanes 2-4*), MKP-1 (*lanes 5-7*), or MKP-3 (*lanes 8-10*) and treated with vehicle (*lanes 2, 5*, and *8*), 50 μmol/L PAO (*lanes 3, 6*, and *9*), or NSC 95397 (*lanes 4, 7*, and *10*). **B,** band intensities were quantitated by luminometry. Lane assignments are identical to **A**. Quantitation data are the averages ± SE from four independent experiments and are presented as percent of GFP-transfected and TPA-stimulated control.

microplate. Cells were classified as positive for chromatin condensation if their average Hoechst intensity exceeded this threshold. Representative images of nuclear morphology were acquired using a 20× objective to better illustrate the phenotype.

Growth Inhibition

Growth inhibition was assessed over a period of 4 days using our previously described high-content cytotoxicity assay (31). Briefly, MDA-MB-231 cells were plated at low density (1,000 per well) in collagen-coated 384-well plates. Cells were treated for 96 h with test agents and fixed for 30 min at room temperature with 4% formaldehyde in HBSS containing 10 μg/mL Hoechst 33342. After two HBSS washes, plates were sealed and nuclei were enumerated by automated batch image acquisition and analysis as described (31).

Isobologram Analysis

Growth inhibition data were analyzed by median-effect analysis using the method of Chou and Talalay (32), where synergism is determined by combination indices (CI) < 1 over a range of effect levels. The CI is defined as $CI = (D)_1 / (Dx)_1 + (D)_2 / (Dx)_2$, where $(Dx)_1$ and $(Dx)_2$ are the concentrations of agents 1 and 2 that produce x% effect and $(D)_1$ and $(D)_2$ are the concentrations of agents 1 and 2 that produce the same x% effect in the presence of the other agent. CI values of <1, 1, and >1 indicate synergism, additivity, and antagonism, respectively.

Results

Inhibition of MKP-1 and MKP-3 by a Quinone-Based DSPase Inhibitor

We examined four quinone-based DSPase inhibitors (Fig. 1A) for cellular inhibition of MKP-1 and MKP-3 by our previously described chemical complementation assay (18, 20, 33). All of these compounds were shown previously to inhibit the DSPase, Cdc25B2, with IC_{50}s < 5 μmol/L (26–28, 34). Cells were transfected in 384-well plates with c-myc-tagged MKP-1 or MKP-3, stimulated with TPA in the presence or absence of test agents, and analyzed by high-content, single-cell analysis for phospho-Erk levels in MKP-expressing and nonexpressing cell subpopulations. In this assay, large differences in Erk phosphorylation between subpopulations indicate high phosphatase activity, whereas small differences indicate low phosphatase activity (20). With a single concentration of 20 μmol/L, we found that only NSC 95397 inhibited MKP-1 and MKP-3 in intact cells (Fig. 1A); the concentration required for a 50% reduction of MKP activity (IC_{50}) was 13 μmol/L for both MKP-1 and MKP-3 (Fig. 1C). *In vitro*, NSC 95397 was a more potent inhibitor of MKP-3 (IC_{50}, 25 ± 12 μmol/L) than MKP-1 (IC_{50}, 65 ± 21 μmol/L). These data suggested that the chemical complementation assay was able to identify compounds not readily detected with homogenous *in vitro* assays using recombinant enzymes and small-molecule substrates.

Verification of MKP-1 Inhibition by NSC 95397 by Western Blot

The multiparameter fluorescence-based assay results were subsequently verified by Western blot analysis. HeLa cells were transfected with MKP-1 or MKP-3 and stimulated with TPA in the presence or absence of 20 μmol/L NSC 95397. Cell lysates were separated on SDS-PAGE and immunoblotted with anti-phospho-Erk and anti-Erk antibodies. Figure 2A shows that, in cells transfected with the phosphatase-inactive GFP, TPA caused an increase in Erk phosphorylation. Expression of either MKP-1 or MKP-3 abrogated that response. Both the broad tyrosine phosphatase inhibitor, phenylarsine oxide (PAO), and NSC 95397 restored Erk phosphorylation in MKP-1- and MKP-3-transfected cells, validating the results from the immunofluorescence assay. Quantification of protein band intensities from four independent experiments confirmed that both PAO and NSC 95397 restored phospho-Erk levels in cells ectopically expressing MKP-1 or MKP-3 (Fig. 2B).

Generation of ROS Is Not Sufficient for MKP Inhibition

Protein tyrosine phosphatases, including MKPs, can be inactivated by generation of ROS, which reversibly oxidize

catalytic cysteines to sulfenic acid derivatives (35, 36). Because all of the compounds tested contained a potentially redox-active *p*-quinone moiety, we investigated whether inhibition of MKP-1 might be a result of ROS generation. Cells were prelabeled for 15 min with the ROS indicator dye, CM-H_2-DCFDA, followed by exposure to test agents for 10 min. Fluorescence micrographs indicated that all agents generated intracellular ROS (Fig. 3A-E). We next quantified the percentage of cells with ROS levels above the average plus 1 SD value of vehicle-treated cells by automated image analysis (Fig. 3F). At a concentration used in the chemical complementation assay (20 μmol/L), JUN-1111, DA-3003-1, and NSC 95397 showed elevated ROS reactivity in 80%, 90%, and 45% of all cells, respectively. NSC 672121 was essentially inactive at this concentration. EC_{50} values were 12.0, 8.3, 25.0, and 30.2 μmol/L for JUN-1111, DA-3003-1, NSC 95397, and NSC 672121, respectively. Because JUN-1111 and DA-3003-1 did not inhibit MKP-1 or MKP-3 despite being potent ROS-generating agents, we conclude that generation of ROS is not sufficient to inhibit cellular MKP-1 and that it seems unlikely that ROS are the main cause for cellular MKP inhibition by NSC 95397.

NSC 95397 Abolishes MKP-1-Mediated Survival Advantage in Human Breast Cancer Cells

Having shown that NSC 95397 inhibited MKP-1 activity in intact cells, we next implemented an experimental system in which cell survival depended on MKP-1. It has been shown previously that the corticosteroid dexamethasone protected cells from paclitaxel-induced apoptosis (11, 12, 37). This effect appears to critically depend on MKP-1, as suppression of MKP-1 expression by small inhibitory RNA (siRNA) restored the apoptotic response of dexamethasone-treated cells to paclitaxel (12). We therefore asked whether NSC 95397 was able to phenocopy the effects of MKP-1 siRNA. MDA-MB-231 cells were pretreated for 1 h with vehicle or dexamethasone (1 μmol/L) followed by 24-h exposure to increasing concentrations of paclitaxel or NSC 95397, respectively. Nuclei were stained with Hoechst 33342 and analyzed for apoptotic nuclear morphology by visual inspection and high-content analysis

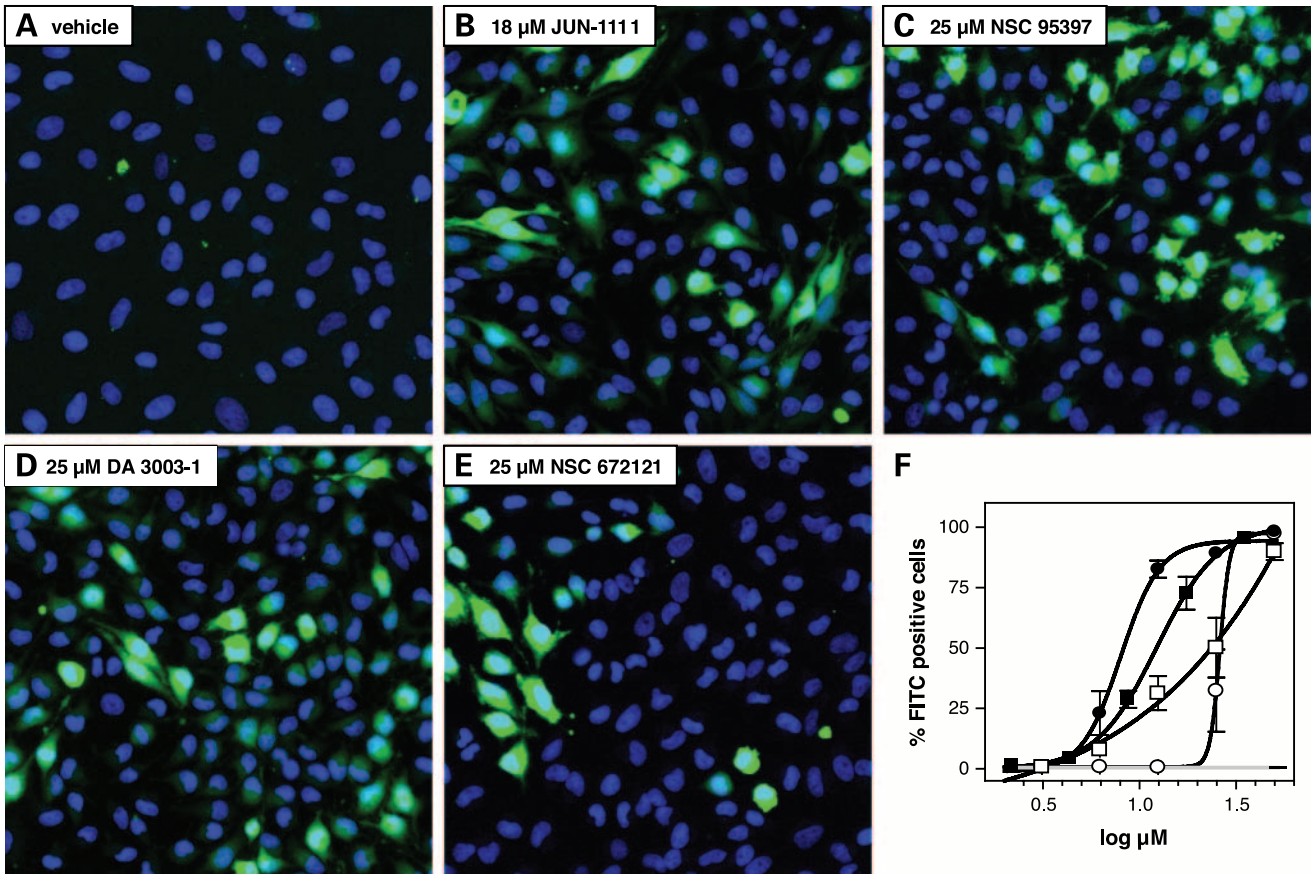

Figure 3. Generation of ROS by quinone-based DSPase inhibitors. Nuclei of confluent HeLa cells were stained with Hoechst 333342. After removal of nuclear stain, cells were preloaded with ROS indicator dye for 10 min followed by a 15-min exposure to test agents. Live cells were imaged by two-channel fluorescence microscopy using a FITC and Hoechst 33342 compatible filter set. **A** to **E,** arbitrarily chosen images of cells treated with vehicle or test agents. **F,** percentages ± SE of ROS-positive cells from triplicate wells treated with vehicle (*gray line*), NSC 672121 (○), DA-3003-1 (●), NSC 95397 (□), or JUN-1111 (■) were calculated by automated image analysis. Data are from a single experiment that has been repeated with similar results.

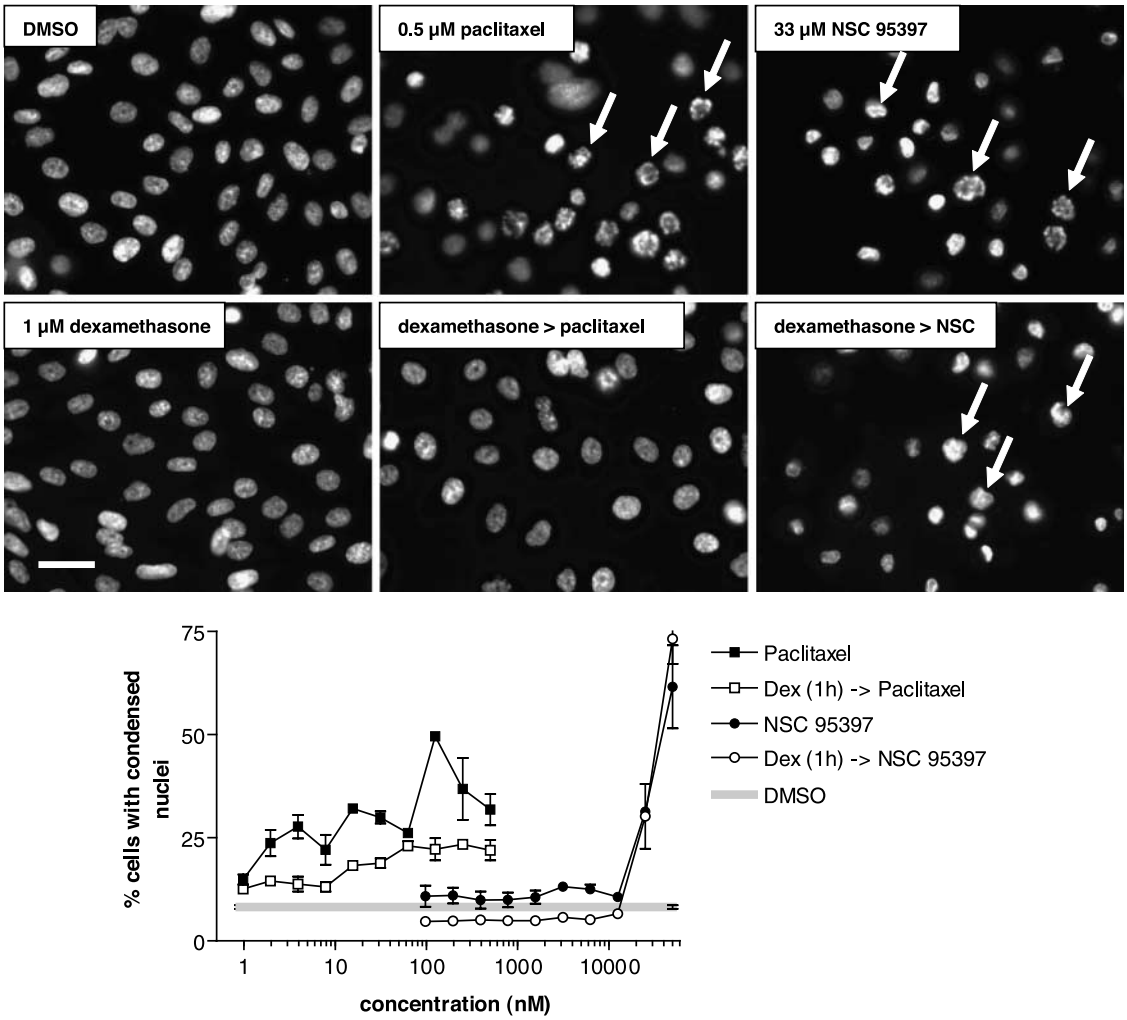

Figure 4. Dexamethasone protects cells against paclitaxel but not NSC 95397–induced apoptosis. MDA-MB-231 cells were pretreated with vehicle (DMSO) or dexamethasone (1 μmol/L) for 1 h followed by increasing concentrations of paclitaxel [DEX (1 h) > paclitaxel] or NSC 95397 [DEX (1 h) > NSC] for an additional 20 h. Nuclei were stained with Hoechst 33342. *Top,* fluorescence photomicrographs of nuclear morphology from a representative imaging field at a single concentration of paclitaxel (0.5 μmol/L) or NSC 95397 (33 μmol/L). *Middle,* nuclear morphology after dexamethasone pretreatment. *Arrows,* nuclei with typical apoptotic morphology. Bar, 25 μm. *Bottom,* quantitative analysis of dexamethasone-mediated cytoprotection. The identical 384-well plate was analyzed for nuclear condensation on an ArrayScan II as described in Materials and Methods. Both paclitaxel and NSC 95397 increased the percentage of cells with condensed chromatin in a concentration-dependent fashion. Dexamethasone pretreatment reduced the percentage of cells with condensed chromatin in cells treated with paclitaxel but not with NSC 95397. Data show the percentage of cells with condensed nuclei and are the averages ± SE from a single experiment that has been repeated twice with similar results.

of condensed nuclei. Consistent with earlier results of Wu et al. (12), paclitaxel caused nuclear morphology changes characteristic of apoptosis (Fig. 4, *top*) that were completely abrogated by dexamethasone pretreatment. In contrast, cells treated with NSC 95397, which also caused nuclear condensation, were unaffected by dexamethasone pretreatment. Quantitative analysis of cells with condensed chromatin by automated microscopy and image analysis confirmed these observations (Fig. 4, *bottom*).

NSC 95397 Restores Paclitaxel Cytotoxicity in Dexamethasone-Protected Cells

We next asked whether NSC 95397 was able to restore apoptosis in cells protected from paclitaxel by dexamethasone. Cells were pretreated for 1 h with dexamethasone alone or a combination of dexamethasone and NSC 95397 followed by exposure to paclitaxel. Figure 5 shows that dexamethasone pretreatment protected cells from paclitaxel-induced apoptosis, confirming the results in Fig. 4 and earlier results (12). Inclusion of a concentration of NSC 95397 (12.5 μmol/L) that approximated the IC_{50} for MKP-1 inhibition in intact cells (see Fig. 1) partially restored apoptosis in dexamethasone-protected cells (Fig. 5A). Similar results were obtained when a higher concentration of NSC 95397 (25 μmol/L) was used (Fig. 5B). Because we have observed previously that NSC 95397 rapidly down-regulated protein levels of the cell cycle phosphatase, Cdc25A (38),

we tested the hypothesis that NSC 95397 might not only inhibit MKP-1 enzyme activity but also decrease MKP-1 protein levels. We found that both dexamethasone and NSC 95397 increased MKP-1 protein levels in MDA-MB-231 cells (Fig. 5C). Thus, the effects of NSC 95397 on dexamethasone cytoprotection could not be explained by a reduction in MKP-1 protein levels.

Combination Cytotoxicity Studies of NSC 95397 and Paclitaxel

At the higher concentration of NSC 95397 used in Fig. 5 (25 μmol/L), it appeared that NSC 95397 accentuated paclitaxel toxicity in the presence of dexamethasone. We therefore investigated whether a combination of NSC 95397 and paclitaxel might be synergistic. We used our previously described growth inhibition assay (31) coupled with an isobologram analysis (32). MDA-MB-231 cells were plated at low density and treated for 4 days with paclitaxel, NSC 95397, or two fixed mixtures of the two agents in the presence or absence of dexamethasone (1 μmol/L). Cell densities at the end of the study were normalized to cell density of vehicle control. Under these conditions, we found IC_{50}, IC_{70}, and IC_{90} values of 8.8, 12.9, and 23.6 nmol/L for paclitaxel and 1.90, 3.15, and 7.09 μmol/L for NSC 95397, respectively. In the presence of dexamethasone, the IC_{50} of paclitaxel was unaffected (8.5 nmol/L), but the IC_{70} and IC_{90} values increased to 15.5 and 40.2 nmol/L, respectively. Consistent with the data in Fig. 4, dexamethasone had a smaller effect on NSC 95397 cytotoxicity, with IC_{50}, IC_{70}, and IC_{90} values of 2.73, 4.42, and 9.49 μmol/L, respectively. Figure 6A and *B* show simulated IC_{50} (*solid line*), IC_{70} (*dotted line*), and IC_{90} (*dashed line*) isoboles for two fixed mixtures of paclitaxel and NSC 95397, where symbols represent measured IC_{50} (●), IC_{70} (□), and IC_{90} (■) values of the two mixtures. In the absence of dexamethasone (Fig. 6A), all combinations with the exception of the 1:250 mixture at the 90% effect level were antagonistic. In the presence of dexamethasone (Fig. 6B), antagonism was converted into additivity at the 50% effect level and into synergism at higher effect levels. CI values, which were calculated for the two mixtures in the presence and absence of dexamethasone as described previously (32), confirmed these results. In the absence of dexamethasone, paclitaxel/

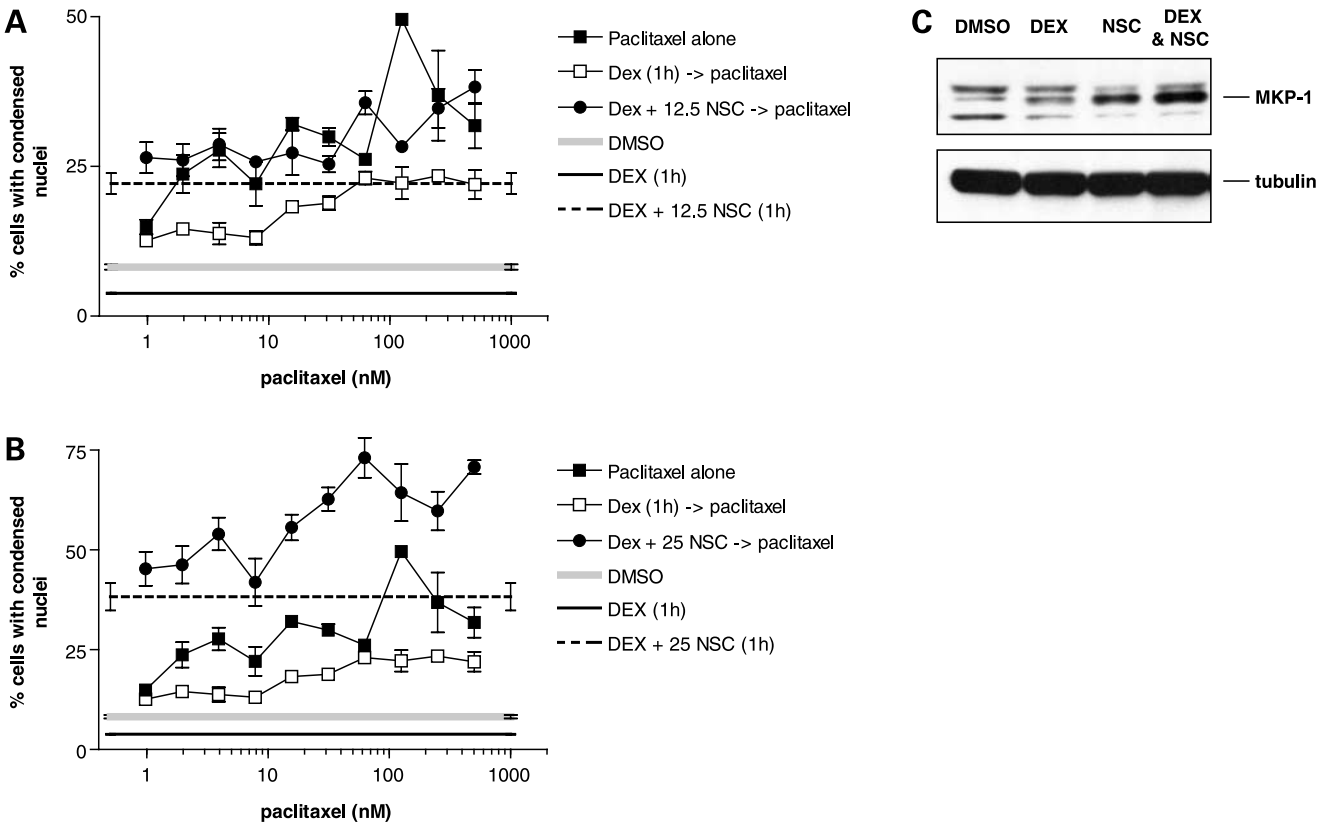

Figure 5. NSC 95397 overrides dexamethasone's cytoprotective effects in paclitaxel-treated cells. MDA-MB-231 cells were pretreated with vehicle, dexamethasone (1 μmol/L), or a mixture of dexamethasone and (**A**) 12.5 μmol/L NSC 95397 or (**B**) 25 μmol/L NSC 95397 for 1 h followed by overnight paclitaxel treatment. Cells with condensed nuclei were quantified on the ArrayScan II. Dexamethasone protected cells against paclitaxel-induced chromatin condensation [□, DEX (1 h) → paclitaxel], and NSC 95397 overrode that effect [●, DEX + NSC → paclitaxel]. Data are from a single experiment that has been repeated twice with similar results. **C,** NSC 95397 does not decrease levels of MKP-1. Lysates from MDA-MB-231 cells treated with vehicle (DMSO), 1 μmol/L dexamethasone (*DEX*), 25 μmol/L NSC 95397 (*NSC*), or a mixture of dexamethasone and NSC 95397 (*DEX & NSC*) were immunoblotted with anti-MKP-1 or anti-α-tubulin antibodies.

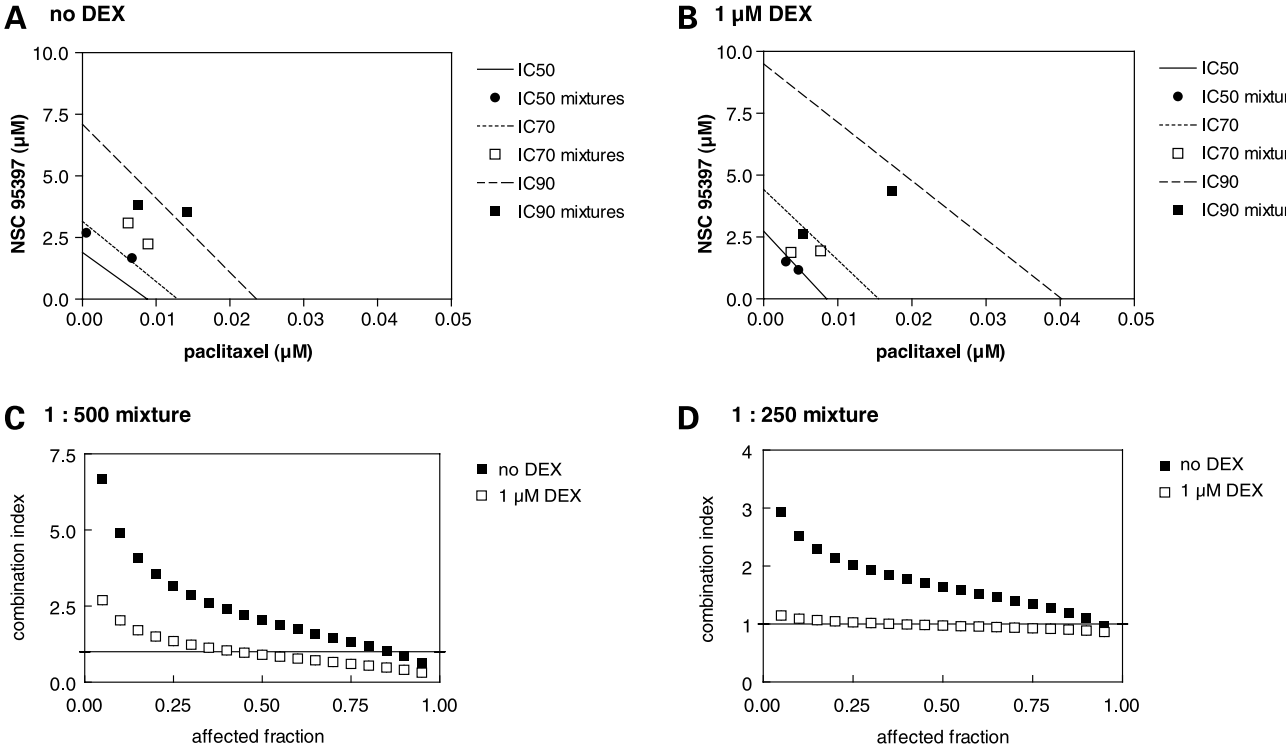

Figure 6. Synergism between paclitaxel and NSC 95397 in the presence of dexamethasone. MDA-MB-231 cells were plated at low density and treated with concentration gradients of paclitaxel, NSC 95397, or mixtures thereof for 4 d in the presence or absence of dexamethasone (1 μmol/L). The percentage of surviving cells was measured as described in Materials and Methods, and data were analyzed by median-effect analysis. **A** and **B,** isobolograms showing IC_{50} (●), IC_{70} (□), and IC_{90} (■) values of two compound mixtures in relation to IC_{50} (*solid line*), IC_{70} (*dotted line*), and IC_{90} (*dashed line*) isoboles, respectively. In the absence of dexamethasone, all data points are at or above their respective isoboles, indicating antagonism. In the presence of dexamethasone, many of the mixtures became synergistic. **C** and **D,** CI values for 1:500 and 1:250 mixtures of paclitaxel and NSC 95397 in the absence (■) or presence (□) of 1 μmol/L dexamethasone. CI values of <1, 1 (*solid line*), and >1 indicate synergism, additivity, and antagonism, respectively. Data were analyzed assuming mutually exclusive drug effects and are from a single experiment that has been repeated twice.

NSC 95397 combinations were antagonistic over the entire range of effect levels. In the presence of dexamethasone, antagonism was converted to additivity at low effect levels and synergism at higher effect levels (Fig. 6C and D). The results robustly repeated over the course of three independent experiments (Table 1).

Discussion

The search for MKP-1 inhibitors with cellular activity has been challenging for a variety of reasons. First, very little structural guidance exists for inhibitor design. In contrast to MKP-3, whose crystal structure has been reported (39), the X-ray structure of MKP-1 has not been solved. Second, performing *in vitro* screens with recombinant MKP-1 has been challenging due to difficulties in producing large amounts of active recombinant enzyme in *Escherichia coli* (19), although a high throughput *in vitro* screen has recently been reported (16). Third, there is considerable ambiguity whether *in vitro* enzyme assays can faithfully reproduce cellular MKP activity. MKPs require interaction with their physiologic protein substrates to become fully active (19, 40). The conformational changes associated with phosphatase-substrate interactions may render assays based on dephosphorylation of small-molecule substrates or short peptides inaccurate predictors of effective phosphatase inhibition in a physiologic context. Cell-based assays, which would permit analysis of MKP-1 activity in a physiologic microenvironment, are impeded because specific cellular readouts for MKP-1 activity do not exist and because MKP-1 has multiple targets in the cell and widely overlapping substrate specificity with other MKPs (1). As a result, cell-active small-molecule inhibitors of MKP-1 are lacking. In their absence, research groups have reluctantly resorted to agents that reduce MKP-1 levels as a side effect, such as anthracyclins (41) or the protein kinase C inhibitor, Ro-31-8220 (42).

We reported previously the development of a definitive cellular assay for MKP inhibition in intact cells (18), which we have coined ''chemical complementation'' (43). The assay is based on the differential measurement of Erk phosphorylation in MKP-expressing and nonexpressing cell subpopulations within the same well of a 384-well microplate. Using this assay, we analyzed four compounds with known DSPase and PTPase inactivating activity for inhibition of MKP-1 and MKP-3. Although all compounds

were structurally similar, shared a *p*-naphthoquinone core structure, and generated ROS, only one of them, that is, NSC 95397, inhibited MKP-1 and MKP-3 in intact cells. The multitargeted nature of NSC 95397 is likely to extend beyond inhibition of MKP-1 and MKP-3, as we know that NSC 95397 inhibits Cdc25A, Cdc25B, and Cdc25C *in vitro* (27), causes cellular phenotypes consistent with Cdc25 inhibition (27, 38), and can activate components of the Erk cascade upstream of MEK (38). We have not yet examined the ability of NSC 95397 to inhibit other MKP family members, but the chemical complementation platform could be adapted to test this in the future.

Within the MKP family, only MKP-1 has been implicated in tumorigenesis. We therefore decided to investigate whether NSC 95397 could phenocopy the effects of MKP-1 siRNA in a cancer-relevant experimental model system dependent on MKP-1 function. We exploited earlier observations by Conzen's group, who reported that chemical induction of MKP-1 by dexamethasone could protect breast cancer cells from paclitaxel-induced apoptosis in culture and *in vivo* (11, 37) and that down-regulation of MKP-1 by siRNA could reverse cytoprotection (11). This experimental system has the added advantage that dexamethasone-mediated cytoprotection is not dependent on MKP-3 because MKP-3 is not induced by dexamethasone (12). Consistent with the hypothesis that inhibition of MKP-1 activity by small molecules might restore sensitivity of dexamethasone-protected cells to paclitaxel, we found that NSC 95397 reversed the antiapoptotic effects of dexamethasone in paclitaxel-treated cells. This effect was not a result of MKP-1 down-regulation, as NSC 95397 did not reduce levels of MKP-1 either by itself or in combination with dexamethasone. Thus, we conclude that inhibition of MKP-1 enzymatic activity is the likely cause for the sensitization of cells to paclitaxel by NSC 95397.

Several research groups have suggested that induction of MKP-1 may limit the activity of chemotherapeutic drugs or radiation therapy (9, 12, 13). To investigate the concept that elimination of MKP-1-mediated cytoprotection may enhance the efficacy of clinically used anticancer agents, we analyzed in detail the interaction of NSC 95397 and paclitaxel by isobologram analysis. Using a 4-day growth inhibition assay, we found that the combination of paclitaxel and NSC 95397, which was antagonistic in the absence of dexamethasone, converted to additivity at low effect levels and to synergism at higher effect levels in the presence of dexamethasone. Thus, inhibition of MKP-1 sensitized cells to paclitaxel only under conditions of MKP-1 up-regulation. This is consistent with the ability of MKP-1 siRNA to restore paclitaxel cytotoxicity in the presence of dexamethasone (12). The observed antagonism between NSC 95397 and paclitaxel in the absence of dexamethasone, however, was unexpected because down-regulation of MKP-1 by siRNA had no effect on paclitaxel-mediated apoptosis unless dexamethasone was present (12) and, in a different cell line, could enhance apoptosis by paclitaxel (44). A possible reason for the antagonistic interaction between paclitaxel and NSC 95397 is that NSC 95397 influences cell cycle arrest by paclitaxel. Paclitaxel cytotoxicity is thought to occur mainly in mitosis, and agents that arrest cells in G_1 reduce paclitaxel toxicity (45). NSC 95397 prevents cell cycle progression through G_1 and G_2 presumably through inhibition of the cell cycle phosphatases Cdc25A, Cdc25B, and Cdc25C (27). It is therefore possible that NSC 95397 reduces paclitaxel toxicity by preventing cells from progressing though G_2-M, and we would predict that a MKP-1-specific inhibitor would not antagonize paclitaxel but instead enhance its activity. This hypothesis will be testable when more selective inhibitors of MKP-1 become available.

Further experiments are needed to determine the precise molecular mechanism by which NSC 95397 inactivates MKP-1 in intact cells. NSC 95397 was not an efficient inhibitor of MKP-1 *in vitro* using an artificial small-molecule substrate. Concentrations of NSC 95397 required to inhibit MKP-1 in our standard, *O*-methyl fluorescein phosphate–based assay for phosphatase activity (27) are about five times higher than those showing cellular activity (IC_{50}, 65 μmol/L). Similarly, Peyregne et al. reported that NSC 95397 activated Erk in intact cells but was unable to inhibit Erk dephosphorylation by recombinant MKP-1 (46). To reconcile the apparent lack of *in vitro* activity with our cellular data, we have attempted to measure phosphatase activity of MKP-1 immunoprecipitated from

Table 1. CI values for fixed mixtures of paclitaxel and NSC 95397 in the presence or absence of dexamethasone

	Paclitaxel/NSC 95397 ratio			
	1:500		1:250	
	No dexamethasone	1 μmol/L dexamethasone	No dexamethasone	1 μmol/L dexamethasone
Effect level*				
ED_{50}	3.47 ± 1.70†	1.08 ± 0.18	2.15 ± 0.44	1.07 ± 0.24
ED_{70}	2.27 ± 0.19	0.88 ± 0.19	1.54 ± 0.21	0.96 ± 0.21
ED_{90}	1.21 ± 0.48	0.64 ± 0.19	0.97 ± 0.11	0.81 ± 0.18

*As determined by 4-day growth inhibition assay in MDA-MB-231 cells.
†Average ± SE combination indices of three independent experiments.

compound-treated HeLa cells as described previously for Cdc25B (28), with the exception that phospho-Erk was used as a substrate in lieu of the artificial phosphatase substrate, *O*-methyl fluorescein phosphate. We were unable to document loss of phosphatase activity in immunoprecipitates from cells treated with NSC 95397, PAO, or sanguinarine, suggesting that none of the agents interacted tightly enough with MKP-1 to keep the immunoprecipitated phosphatase in an inactive state during isolation (data not shown). Because PAO and sanguinarine are thought to covalently modify protein thiols, their lack of activity indicates that this type of assay is not suited to measure inhibition of cellular MKP-1. A possible explanation for the discrepancy between the *in vitro* and cellular activities is that NSC 95397 could indirectly affect MKP-1 phosphatase activity, similar to what has become known in the protein kinase field as ''noncatalytic inhibitors'' (47). Such a mechanism of action could involve inactivation of an activator of MKP-1 or preventing the association of MKP-1 with its respective substrates or activating proteins. It is also possible that *in vitro* phosphatase assays do not faithfully recapitulate conditions required for cellular protein dephosphorylation. For example, PAO is considerably less active *in vitro* compared with cultured cells (48). In our hands, PAO also had cellular activity in the low micromolar range (18) but was inactive against purified recombinant MKP-1 protein (IC_{50} > 350 μmol/L; data not shown).

Despite its multitargeted nature, NSC 95397 had cellular effects consistent with MKP-1 inhibition in experimental model systems of MKP-1-dependent cell growth and survival. The data provide for the first time evidence that a small-molecule antagonist of MKP-1 can produce effects similar to those seen with siRNA and support the hypothesis that MKP-1 inhibition by small molecules could enhance the therapeutic efficacy of conventional anticancer therapies. The results underscore the need to discover and develop more potent, selective, and cell-active inhibitors of this elusive enzyme.

Acknowledgments

We thank Nicholas Walrath and Drew Kirschmann for excellent technical assistance.

References

1. Farooq A, Zhou M-M. Structure and regulation of MAPK phosphatases. Cell Signal 2004;16:769 – 79.

2. Keyse SM. Protein phosphatases and the regulation of mitogen-activated protein kinase signalling. Curr Opin Cell Biol 2000;12:186 – 92.

3. Sun H, Charles CH, Lau LF, Tonks NK. MKP-1 (3CH134), an immediate early gene product, is a dual specificity phosphatase that dephosphorylates MAP kinase *in vivo*. Cell 1993;75:487 – 93.

4. Brondello JM, Pouyssegur J, McKenzie FR. Reduced MAP kinase phosphatase-1 degradation after p42/p44MAPK-dependent phosphorylation. Science 1999;286:2514 – 7.

5. Marchetti S, Gimond C, Chambard JC, et al. Extracellular signal-regulated kinases phosphorylate mitogen-activated protein kinase phosphatase 3/DUSP6 at serines 159 and 197, two sites critical for its proteasomal degradation. Mol Cell Biol 2005;25:854 – 64.

6. Ducruet AP, Vogt A, Wipf P, Lazo JS. Dual specificity protein phosphatases: therapeutic targets for cancer and Alzheimer's disease. Annu Rev Pharmacol Toxicol 2005;45:725 – 50.

7. Liao Q, Guo J, Kleeff J, et al. Down-regulation of the dual-specificity phosphatase MKP-1 suppresses tumorigenicity of pancreatic cancer cells. Gastroenterology 2003;124:1830 – 45.

8. Franklin CC, Srikanth S, Kraft AS. Conditional expression of mitogen-activated protein kinase phosphatase-1, MKP-1, is cytoprotective against UV-induced apoptosis. Proc Natl Acad Sci U S A 1998;95:3014 – 9.

9. Sanchez-Perez I, Martinez-Gomariz M, Williams D, Keyse SM, Perona R. CL100/MKP-1 modulates JNK activation and apoptosis in response to cisplatin. Oncogene 2000;19:5142 – 52.

10. Wang Z, Xu J, Zhou JY, Liu Y, Wu GS. Mitogen-activated protein kinase phosphatase-1 is required for cisplatin resistance. Cancer Res 2006;66:8870 – 7.

11. Wu W, Chaudhuri S, Brickley DR, et al. Microarray analysis reveals glucocorticoid-regulated survival genes that are associated with inhibition of apoptosis in breast epithelial cells. Cancer Res 2004;64:1757 – 64.

12. Wu W, Pew T, Zou M, Pang D, Conzen SD. Glucocorticoid receptor-induced MAPK phosphatase-1 (MKP-1) expression inhibits paclitaxel-associated MAPK activation and contributes to breast cancer cell survival. J Biol Chem 2005;280:4117 – 24.

13. Small GW, Shi YY, Edmund NA, et al. Evidence that mitogen-activated protein kinase phosphatase-1 induction by proteasome inhibitors plays an antiapoptotic role. Mol Pharmacol 2004;66:1478 – 90.

14. Nyati MK, Feng FY, Maheshwari D, et al. Ataxia telangiectasia mutated down-regulates phospho-extracellular signal-regulated kinase 1/2 via activation of MKP-1 in response to radiation. Cancer Res 2006;66: 11554 – 9.

15. Lazo JS, Nunes R, Skoko JJ, et al. Novel benzofuran inhibitors of human mitogen-activated protein kinase phosphatase-1. Bioorg Med Chem 2006;15:5643 – 50.

16. Johnston PA, Foster CA, Shun TY, et al. Development and implementation of a 384-well homogeneous fluorescence intensity high-throughput screening assay to identify mitogen-activated protein kinase phosphatase-1 dual-specificity protein phosphatase inhibitors. Assay Drug Dev Technol 2007;5:319 – 32.

17. Lazo JS, Skoko JJ, Werner S, et al. Structurally unique inhibitors of human mitogen-activated protein kinase phosphatase-1 identified in a pyrrole carboxamide library. J Pharmacol Exp Ther 2007;322:940 – 7.

18. Vogt A, Tamewitz A, Skoko J, et al. The benzo(*c*)phenanthridine alkaloid, sanguinarine, is a selective, cell-active inhibitor of mitogen-activated protein kinase phosphatase-1. J Biol Chem 2005;280: 19078 – 86.

19. Chen P, Hutter D, Liu P, Liu Y. A mammalian expression system for rapid production and purification of active MAP kinase phosphatases. Protein Expr Purif 2002;24:481 – 8.

20. Vogt A, Cooley KA, Brisson M, et al. Cell-active dual specificity phosphatase inhibitors identified by high-content screening. Chem Biol 2003;10:733 – 42.

21. Chaturvedi MM, Kumar A, Darnay BG, et al. Sanguinarine (pseudochelerythrine) is a potent inhibitor of NF-κB activation, IκBα phosphorylation, and degradation. J Biol Chem 1997;272:30129 – 34.

22. Eun JP, Koh GY. Suppression of angiogenesis by the plant alkaloid, sanguinarine. Biochem Biophys Res Commun 2004;317:618 – 24.

23. Tanaka S, Sakata Y, Morimoto K, et al. Influence of natural and synthetic compounds on cell surface expression of cell adhesion molecules, ICAM-1 and VCAM-1. Planta Med 2001;67:108 – 13.

24. Adhami VM, Aziz MH, Reagan-Shaw SR, et al. Sanguinarine causes cell cycle blockade and apoptosis of human prostate carcinoma cells via modulation of cyclin kinase inhibitor-cyclin-cyclin-dependent kinase machinery. Mol Cancer Ther 2004;3:933 – 40.

25. Nishikawa Y, Carr BI, Wang M, et al. Growth inhibition of hepatoma cells induced by vitamin K and its analogs. J Biol Chem 1995;270: 28304 – 10.

26. Lazo JS, Aslan DC, Southwick EC, et al. Discovery and biological evaluation of a new family of potent inhibitors of the dual specificity protein phosphatase Cdc25. J Med Chem 2001;44:4042 – 9.

27. Lazo JS, Nemoto K, Pestell KE, et al. Identification of a potent and selective pharmacophore for Cdc25 dual specificity phosphatase inhibitors. Mol Pharmacol 2002;61:720 – 8.

28. Brisson M, Nguyen T, Wipf P, et al. Redox regulation of Cdc25B by cell-active quinolinediones. Mol Pharmacol 2005;68:1810 – 20.

29. Groom LA, Sneddon AA, Alessi DR, Dowd S, Keyse SM. Differential

regulation of the MAP, SAP and RK/p38 kinases by Pyst1, a novel cytosolic dual-specificity phosphatase. EMBO J 1996;15:3621 – 32.

30. Dowd S, Sneddon AA, Keyse SM. Isolation of the human genes encoding the pyst1 and Pyst2 phosphatases: characterisation of Pyst2 as a cytosolic dual-specificity MAP kinase phosphatase and its catalytic activation by both MAP and SAP kinases. J Cell Sci 1998;111:3389 – 99.

31. Vogt A, Kalb EN, Lazo JS. A scalable high-content cytotoxicity assay insensitive to changes in mitochondrial metabolic activity. Oncol Res 2004;14:305 – 14.

32. Chou TC, Talalay P. Quantitative analysis of dose-effect relationships: the combined effects of multiple drugs or enzyme inhibitors. Adv Enzyme Regul 1984;22:27 – 55.

33. Vogt A, Lazo JS. Discovery of protein kinase phosphatase inhibitors. Methods Mol Biol 2006;356:389 – 400.

34. Tamura K, Southwick EC, Kerns J, et al. Cdc25 inhibition and cell cycle arrest by a synthetic thioalkyl vitamin K analogue. Cancer Res 2000; 60:1317 – 25.

35. Salmeen A, Andersen JN, Myers MP, et al. Redox regulation of protein tyrosine phosphatase 1B involves a sulphenyl-amide intermediate. Nat Struct Biol 2003;423:769 – 73.

36. Kamata H, Honda S, Maeda S, et al. Reactive oxygen species promote TNFα-induced death and sustained JNK activation by inhibiting MAP kinase phosphatases. Cell 2005;120:649 – 61.

37. Pang D, Kocherginsky M, Krausz T, Kim SY, Conzen SD. Dexamethasone decreases xenograft response to paclitaxel through inhibition of tumor cell apoptosis. Cancer Biol Ther 2006;5:933 – 40.

38. Nemoto K, Vogt A, Oguri T, Lazo JS. Activation of the Raf-1/MEK/Erk kinase pathway by a novel Cdc25 inhibitor in human prostate cancer cells. Prostate 2004;58:95 – 102.

39. Stewart AE, Dowd S, Keyse SM, McDonald NQ. Crystal structure of the MAPK phosphatase Pyst1 catalytic domain and implications for regulated activation. Nat Struct Biol 1999;6:174 – 81.

40. Camps M, Nichols A, Gillieron C, et al. Catalytic activation of the phosphatase MKP-3 by ERK2 mitogen-activated protein kinase. Science 1998;280:1262 – 5.

41. Small GW, Somasundaram S, Moore DT, Shi YY, Orlowski RZ. Repression of mitogen-activated protein kinase (MAPK) phosphatase-1 by anthracyclines contributes to their anti-apoptotic activation of p44/42-MAPK. J Pharmacol Exp Ther 2003;307:861 – 9.

42. Mizuno R, Oya M, Shiomi T, et al. Inhibition of MKP-1 expression potentiates JNK related apoptosis in renal cancer cells. J Urol 2004;172: 723 – 7.

43. Vogt A, Takahito A, Ducruet AP, et al. Spatial analysis of key signaling proteins by high-content solid-phase cytometry in Hep3B cells treated with an inhibitor of Cdc25 dual-specificity phosphatases. J Biol Chem 2001;276:20544 – 50.

44. Small GW, Shi YY, Higgins LS, Orlowski RZ. Mitogen-activated protein kinase phosphatase-1 is a mediator of breast cancer chemoresistance. Cancer Res 2007;67:4459 – 66.

45. Johnson KR, Wang L, Miller MC III, Willingham MC, Fan W. 5-Fluorouracil interferes with paclitaxel cytotoxicity against human solid tumor cells. Clin Cancer Res 1997;3:1739 – 45.

46. Peyregne VP, Kar S, Ham SW, et al. Novel hydroxyl naphthoquinones with potent Cdc25 antagonizing and growth inhibitory properties. Mol Cancer Ther 2005;4:595 – 602.

47. Wesche H, Xiao SH, Young SW. High throughput screening for protein kinase inhibitors. Comb Chem High Throughput Screen 2005;8: 181 – 95.

48. Noguchi T, Matozaki T, Horita K, Fujioka Y, Kasuga M. Role of SH-PTP2, a protein-tyrosine phosphatase with Src homology 2 domains, in insulin-stimulated Ras activation. Mol Cell Biol 1994;14:6674 – 82.